FER Regression Analysis of DS-UWB-based WPAN

F. De Rango[1], F. Veltri[1], P. Fazio[1], A. F. Santamaria[2], M. Tropea[1], Salvatore Marano[1]
D.E.I.S. Department, University of Calabria, Italy, 87036
[1]e-mail: {derango, fveltri, pfazio, mtropea, marano}@deis.unical.it
[2]santamaria@si.deis.unical.it.it

Abstract

Ultra-Wideband (UWB) technology is at present defined as any wireless transmission scheme that occupies a fractional bandwidth ≥20%, or more than 500 MHz of absolute bandwidth. In this paper we have considered an UWB system, based on Direct Sequence - UWB (DS-UWB) proposal standard, in an indoor multipath environment modeled in accordance with IEEE 802.15 channel modeling subcommittee. Performance are evaluated in terms of Frame Error Rate (FER) vs. transmitter-receiver distance and frame size and finally a polynomial regression analysis is carried out on simulation results in order to obtain a closed formula to describe, for different scenarios, the FER as a function of data rates, frame size and distance between transmitter and receiver.

Index Terms—UWB, DS-UWB, MMSE, IEEE 802.15.3a.

1. Introduction

In the last few years, Ultra-Wideband communication systems have been extensively studied in both the computer and communication communities. UWB technology is at present defined by the *Federal Communications Commission* (FCC) as any wireless transmission scheme that occupies a fractional bandwidth ≥20%, or more than 500 MHz of absolute bandwidth [1].

The potential strength of the UWB-radio technique lies in its use satisfying desirable capabilities including: accurate position location and ranging, and lack of significant multi-path fading owing to fine delay resolution; multiple access owing to wide transmission bandwidths; communications becoming confused with background noise owing to low transmission power operation; possible easier material penetration owing to the low frequency components.

Due to these technical advantages and to recent commercial interest, IEEE founded the task group 802.15.3a in order to standardize a physical layer for UWB communications systems [2]. Two standards have become the most considered in the academic and industrial environment in the last few years: DS-UWB [3] and *Multi Band - Orthogonal Frequency Division Multiplexing* (MB-OFDM). In this work, we focus our attention on the DS-UWB proposal standard, so, in accordance with [4], we have modeled a DS-UWB system in order to evaluate its performances. However, our main contribution, which is the novel element provided, is not to analyze the performance of DS-UWB system already investigated in previous works, even if with respect to [4] we have also considered the different dimension of the frame length and carried out our analysis varying the channel scenario and frame size, but it is still a three-variables regression analysis in order to obtain a closed formula to describe, for different scenarios, the FER as a function of data rates, frame size and distance between transmitter and receiver. In particular, starting by simulation results, we well explained our analytic approach step by step and therefore two specific cases are shown in order to provide three variables functions of FER for *Line Of Sight* (LOS) and No-*Line Of Sight* (NLOS) scenarios.

In the following a brief description of the transmitter and receiver structure and of the channel model is made in section 2; related works are presented in section 3; performance evaluation and regression analysis are show in section 4; while conclusions are drawn in section 5.

2. DS-UWB Architecture

In this section, a brief description of the DS-UWB architecture and sequential operations effectuated on the data will be made. Furthermore, IEEE channel model and the introduction of distance dependence will be explained.

2.1. Transmitter and Receiver Structure

DS-UWB realizes a *Wireless Personal Area Network* (WPAN) with a very high data payload communication capabilities. As described in the standard [3], the data sequence is scrambled in order to ensure an adequate number of bit transitions to support clock recovery. Then, a convolutional encoder is used to encode data so that the decoder can correct errors, due to noise, introduced in the channel. In particular, we use a convolutional encoder with a constraint length k=6 (that is an encoder in which the number of inputs in the encoder diagram is 6) that realizes a code rate of ½. Instead, the other code rates are obtained using the puncturing technique (some of the encoded bits are omitted in the transmission increasing in this way the coding rate). Therefore, the encoded data are interleaved with a convolutional interleaver in order to disperse burst errors to which the decoder is sensitive and then modulated using *Binary Phase Shift Keying* (BPSK) modulation. Each modulated bit is successively spreaded using a ternary *Pseudo Noise* (PN) spreading code to form the transmition sequence. The combination of the *spreading factor*, SF, (that is the length of the spreading code), the code rate and used modulation forms the current data rate.

The receiver structure is instead organized as follows: the transmitted bit sequence is estimated using a *Minimum Mean Square Error* (MMSE) receiver, because it is more effective than a four or eight fingered RAKE at multipath combining

and its complexity is constant, as described in [9]. This receiver uses an adaptive algorithm called *Normalised Least Minimum Square* (NLMS) to upgrade weights vector *W*. The equation to calculate the weights is specified below. For more details refer to [9].

$$W(i) = W(i-1) + \mu_m e(i) \frac{u^*(i)}{\varepsilon + u^H(i)u(i)} \quad (1)$$

In equation (1), μ_m is the step size, while ε is a small positive constant that has been added (to denominator) to overcome potential numerical instability in the update of the weights; *e(i)* is the error associated with the *i-th* estimated bit; *u(i)* represents the discrete input signal of the adaptive filter. After this operation, the estimated bits are demodulated and deinterleaved and successively are sent in a Viterbi decoder, which recovers some of the errors introduced by the channel. The decoded bits are finally descrambled in order to reconstruct the data sequence.

In our simulations, we use an MMSE receiver with 16 taps per observation window and a step size of 0.5.Moreover, we work in the piconet channel 1 of the lower band with a chip rate of 1313 MHz and, for every simulation campaign, we fixed the transmission power to -25 dB.

TABLE I
Channel Characteristics

Scenario	CM1	CM2	CM3	CM4
Mean Excess Delay (nsec)	5.0	9.9	15.9	30.1
RMS delay spread (nsec)	5.0	8.0	15.0	25.0
Number of paths within 10 dB of peak	12.5	15.3	24.9	41.2
Number of pats with 80% of energy	20.8	33.9	64.7	123.3
Energy mean (dB)	-0.4	-0.5	0	0.3
Energy standard deviation (dB)	2.9	3.1	3.1	2.7

2.2. Channel Model

In our simulator, we utilize the UWB channel model provided by IEEE 802.15 channel modeling subcommittee [8]. As the channel measurements showed multipaths arriving in clusters, this model for the time-of-arrival statistics uses the *Saleh-Valenzuela* approach [6]. The model proposed in [8] provides four different multipath fading scenario: CM1 (that describes a *Line of Sight*, LOS, scenario), CM2 and CM3 (that describe two different *No-Line of Sight*, NLOS, scenarios) and CM4 (that depicts a very extreme NLOS scenario). The shadowing effect is also included in the model and it is assumed to be common to all environments (in particular, it is modeled as a lognormal distribution with a log-standard deviation of 3 dB). The main characteristics of the channel model are summarized in Table I. Further details can be found in [8].

In accordance with [4], a free path loss model is also employed. In particular, the path loss for the distance between transmitter and receiver $d \geq 1\ m$ is given by:

$$PL(d) = 20\log_{10}\left(\frac{4 \cdot \pi \cdot d \cdot f_c}{c}\right), \quad f_c = \sqrt{f_{\min} \cdot f_{\max}} \quad (2)$$

where f_c is the geometric centre frequency, with f_{min} and f_{max} being the lower and the upper -10 dB cutoff frequencies of the power spectrum, and *c* is the light speed. As in [4], we incorporate the equation (2) in each channel realization in order to account the distance dependence. In particular, using (2), each path is attenuated by a factor depending on the distance really covered: this distance is computed on the basis of needed time to reach the receiver under the assumption that the path speed is the light speed.

3. Related Work

In the last few years many works have been realized on the channel modeling of UWB networks. In particular these approaches considered the main phenomena affecting wireless communications such as multipath fading, shadowing and path loss ([5],[6],[7],[8]). Furthermore research have been demonstrated as in the UWB channel the paths follow a cluster-based arrival rate. These characteristics are different from the classical IEEE 802.11 wireless networks channel models. This approach is first adopted in the Saleh-Valenzuela (S-V) model where the path arrival times are modeled through two Poisson distributions, where the first one is used to model the arrival time of the first path in each cluster, while the second one describes the arrival time of other paths in each cluster [6]. The path amplitudes follow a Rayleigh distribution law, with a double exponential decay model. Subsequently the S-V model has been extended in [8] where the authors propose a log-normal distribution to approximate the amplitudes of the power associated with the path components. However, in [8], the impulse response is not explicitly associated with the transmitter-receiver distance. Thus, following the model presented in [8], which is the formal model adopted by IEEE 802.15.3a, it is possible to account for the distance dependence modifying the first path time arrival and further attenuating other paths on the basis of the covered distance.

Another important aspect of UWB communication is the receiver structure: in many works it has been proofed that a simply RAKE receiver is not sufficient to explore the total energy of the paths due to dense multipath typical of UWB channel. In this contest, an important role is taken by *Minimum Mean Square Error* (MMSE) receiver: in particular in [10], the authors described the MMSE equalization: *linear equalization* (LE) and *decision feedback equalization* (DFE) are analyzed. LE and DFE are both suitable choices for the DS-UWB system even if DFE has a better performance for high date rate, but equalization is also more complex in this case. In [4] and [10] the authors combine the RAKE receiver and the MMSE equalization to recover the transmitted signal, but in [9] is shown that the MMSE receiver alone can be sufficient to recover the data. In order to reduce the receiver

complexity, in our model we use only the MMSE receiver with a linear equalization.

Finally, a performance evaluation of DS-UWB system has already carried out in [4], but in this analysis no assumptions are made on the frame length. In our work, instead, we introduced different frame dimensions , so we carried out our analysis varying the channel scenario and frame size. However, the very novel element of this contribution is a three-variables regression analysis in order to obtain a closed formula to describe, for different scenarios, the FER as a function of data rates, frame size and distance between transmitter and receiver.

4. Performance Evaluation

Many simulation campaigns have been carried out in order to evaluate the performance of the DS-UWB physical layer for the UWB technology. Simulation results and regression analysis will be presented in the following.

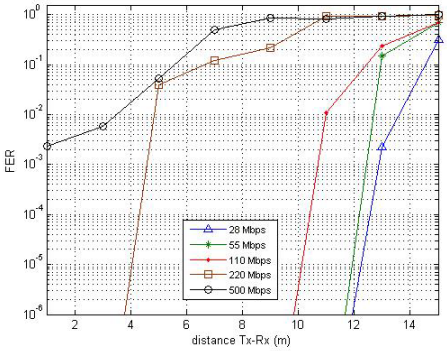

Fig.1. FER vs. distance for CM1 scenario with a frame size of 128 bytes.

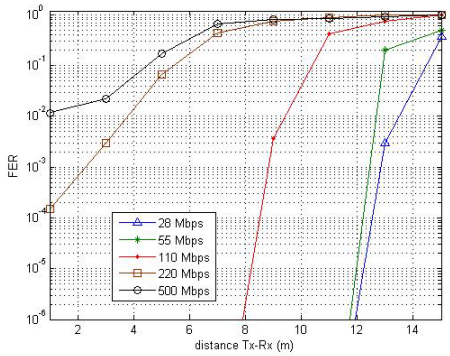

.

Fig.2. FER vs. distance for CM1 scenario, frame size of 1024 bytes.

4.1. Simulation Results

Our simulation campaigns confirm the results obtained in [3] and show how the UWB systems are very sensitive to the transmitter-receiver distance and how the frame size can influences the system performances decreasing the operative range in some cases. Owing to lack of space, in this paper we show and analyze only the results for CM1 and CM2 scenario with a frame length of 128 and 1024 bytes.

Generally, we can observe how, only the lower data rates (28, 55, 110 Mbps) allow transmission over a sufficiently long distance, whereas other data rates (220 Mbps and 500 Mbps) are more sensitive to the distance. In fact, low rates reject *inter-symbol interference* (ISI) better than the higher rates because of longer spreading codes, which have more zero-valued windows than a shorter sequence in their autocorrelation function, so interference owing to multipaths that are within these windows can be eliminated. These performance differences are more pronounced for the CM2 scenario because, in this case, the absence of a stronger direct component makes the impact of the ISI more damaging.

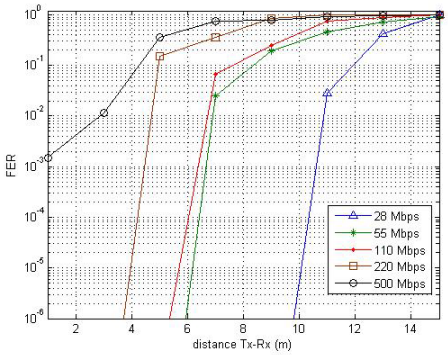

Fig.3. FER vs. distance for CM2 scenario with a frame size of 128 bytes.

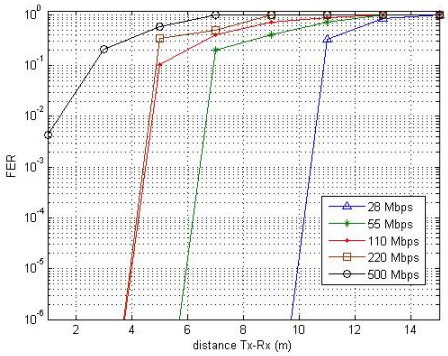

Fig.4. FER vs. distance for CM2 scenario with, frame size of 1024 bytes.

In Fig.1 and Fig.2 the curves of average FER in a CM1 scenario for 28, 55, 110, 220, 500 Mbps data rates and for two different frame size (128 bytes in Fig.1 and 1024 bytes in Fig.2) are plotted. Typically, the FER, as demonstrated in [11], is a function of the BER distribution but it is also a function of the frame sizes, therefore if the frame size is made to go towards one (degenerate case) the FER converges towards the BER, vice versa at an increase of the frame size the FER tends to one. This trend is also confirmed for the DS-UWB systems, in fact we can see how the FER for 1024 bytes frame size is greater than FER obtained for 128 bytes. This aspect is very important for a UWB system because an increase of FER can reduce the operative range of a certain data rate (we remember that the operative range is the distance for which FER<0.08 with 90% probability). In particular, we

can see how the operative range of 110 Mbps decreases from 11.6 meters, obtained for a frame size of 128 bytes, to 9.4 meters obtained for 1024 bytes. Instead, we observe that lower data rates (28 and 55 Mbps) are less sensitive to frame size and so the operative range decreases.

Fig.3 and Fig.4 show the curves of average FER in a CM2 scenario for 28, 55, 110, 220, 500 Mbps data rates and for 128 bytes frame size (in Fig.3) and for 1024 bytes frame (in Fig.4). In this case, the increase of frame dimension also affects lower data rates: e.g. we can see how the 28 Mbps operative range reduce up to 9.5 meters for a dimension of 1024 bytes, whereas for 55 Mbps we observe an operative range reduction of about 2 meters (from 7.7 meters for a frame size of 128 bytes to 6 meters obtained for a frame of 1024 bytes).

In Table II, we summarize the operative range for all data rates in the CM1 and CM2 scenarios with a frame size of 128 bytes and of 1024 bytes.

TABLE II
Operative Range for DS-UWB (in meters)

Data Rate	CM1 (128 B)	CM1 (1024 B)	CM2 (128 B)	CM2 (1024 B)
28 Mbps	13.5	13.4	11.3	9.5
55 Mbps	12.1	11.8	7.7	6
110 Mbps	11.6	9.4	7	4.5
220 Mbps	6.5	5.1	4.2	3.5
500 Mbps	5.1	3.7	3.4	1.8

4.2. FER Regression Analysis

In order to obtain an expression for the average FER as a function of the distance d (in meters), the frame size p (in byte) and data rate r (in Mbps) a regression analysis has been carried out, on the simulation results, using the Mathworks's Matlab tool.

The regression analysis is an interpolation procedure providing a function fitting data point obtained from simulation, so simulation campaigns are necessary to carry it out. However, the obtained expressions can be considered as closed formulas because they describe the FER trend in the given ranges of distance and frame length; moreover, these functions can be used in future work without the need of further physical layer simulations (this feature is a very important contribution). In this work, we perform a polynomial regression analysis on the FER logarithm, so we obtain exponential functions: details on regression technique and how to carry it out can be found in [12]. Generally, the goodness of a regression analysis can be confirmed by two distinct indexes: the *determination coefficient* R^2 and the *relative error percentage* [11]. R^2 can take on any value between 0 and 1, with a value closer to 1 indicating that a greater proportion of variance is accounted by the model (e.g. R^2 value of 0.8234 means that the fit explains 82.34% of the total variation in the data about the average). The *determination coefficient* R^2 is given by:

$$R^2 = 1 - \frac{SSE}{SST} \tag{3}$$

where the *Sum of Squares due to Error* (*SSE*) and the *Sum of Squares about the Mean* (*SST*) are respectively defined as:

$$\begin{aligned} SSE &= \left\| y - \hat{y} \right\|^2 \\ SST &= \left\| y - \overline{y} \right\|^2 \end{aligned} \tag{4}$$

In the previous formulas, the operator $\left\| \cdot \right\|$ represents the *Euclideal Norm*, y is the ordinate simulated data point vector, $\hat{y}$ is the resulting fit data point vector, while $\overline{y}$ is the mean value of vector y.

The *relative error percentage* is instead defined as:

$$e_{rel} = \left| \frac{y - \hat{y}}{y} \right| \times 100 \tag{5}$$

In this case, the polynomial approximation is considered good if the relative error is less than 8% for each data point.

As described above, since the FER assumes very low values in some cases (e.g. for a short distance, specifically for the CM1 scenario), we carried out the regression analysis on the FER logarithm in this way reducing, the percentage of error.

The general equation of the logarithm of FER, for a fixed data rate and frame size, can be expressed with a n-th order polynomial regression:

$$\log_{10}\left[FER(d)\right] = (a_n d^n + \ldots + a_3 d^3 + a_2 d^2 + a_1 d + a_0) \tag{6}$$

where $a_i = f(p)$ with $i=0,1,\ldots n$.

Therefore the average FER can be represented in the following way:

$$FER(d) = 10^{\left(\begin{bmatrix} a_0 & a_1 & \cdots & a_n \end{bmatrix} \begin{bmatrix} 1 \\ d \\ \vdots \\ d^n \end{bmatrix} \right)} = 10^{\langle a \rangle \cdot \langle d \rangle_n^T} \quad 1m < d \le 15m \tag{7}$$

where the notation $\langle \cdot \rangle$ is used to represent a row vector and $\langle \cdot \rangle^T$ is the transpose operator applied to the vector. In equation (7) $\langle d \rangle_n^T$ is a $(n+1)\times 1$ vector.

Considering another polynomial regression analysis on the a_i coefficients for different p values of frame size, the polynomial expression of the a_i terms can be represented as follows:

$$a_i(p) = b_{m,i} p^m + \ldots + b_{2,i} p^2 + b_{1,i} p + b_{0,i} \tag{8}$$

with $i=0,\ldots,n$.

Therefore the coefficients of the frame size can be expressed in the following way:

$$\langle a(p) \rangle = \begin{bmatrix} b_{0,0} & b_{0,1} & \ldots & b_{0,m} \\ b_{1,0} & \ldots & \ldots & \ldots \\ \ldots & \ldots & \ldots & \ldots \\ b_{n,0} & \ldots & \ldots & b_{n,m} \end{bmatrix} \cdot \begin{bmatrix} 1 \\ p \\ \vdots \\ p^m \end{bmatrix} = B \cdot \langle p \rangle_m^T \tag{9}$$

Where $\langle p \rangle_m^T$ represent a $(m+1)\times 1$ vector.

A third regression is finally carried out on each coefficient of B, introducing in this way also the dependence on data rate r.

Therefore the coefficients of matrix B can be expressed as:

$$b_{i,j}(r) = c_{m',(i,j)} r^{m'} + \ldots + c_{2,(i,j)} r^2 + c_{1,(i,j)} r + c_{0,(i,j)} \qquad (10)$$

Substituting equation (10) in (9) for each coefficient, we obtain the following formula:

$$\langle a(p,r) \rangle = \begin{bmatrix} b_{0,0}(r) & b_{0,1}(r) & \ldots & b_{0,m}(r) \\ b_{1,0}(r) & \ldots & \ldots & \ldots \\ \ldots & \ldots & \ldots & \ldots \\ b_{n,0}(r) & \ldots & \ldots & b_{n,m}(r) \end{bmatrix} \cdot \begin{bmatrix} 1 \\ p \\ \vdots \\ p^m \end{bmatrix} = B(r) \cdot \langle p \rangle_m^T \qquad (11)$$

In (10) and (11), the polynomials $b_{i,j}(r)$ and the degrees m, m' and n depend on considered scenario (CM1, CM2, CM3 or CM4). Substituting (11) within (7), the following equation can be obtained:

$$\begin{aligned} &FER(d,p,r) = 10^{\left(\left[B(r)\cdot\langle p\rangle_m^T\right]\langle d\rangle_n^T\right)}; \\ &1m \le d \le 15m;\ 128bytes \le p \le 1024bytes; \\ &r \in [28Mbps,\ 55Mbps,\ 110Mbps,\ 220Mbps,\ 500Mbps]; \end{aligned} \qquad (12)$$

where the $FER = f(d,p,r)$.

Equation (12) is a general formula useful for all scenarios. In the following some examples of these functions for a fixed data rate and scenario are shown.

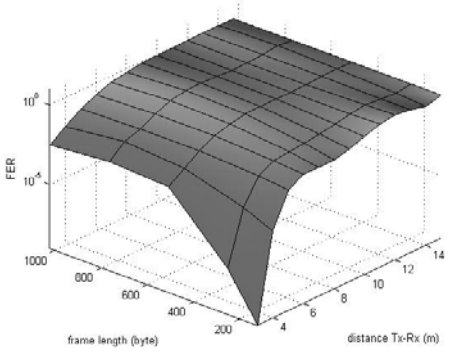

(a)

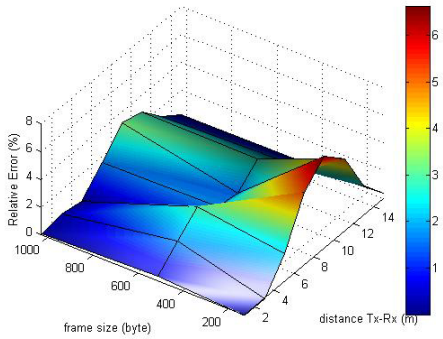

(b)

Fig.5.a) FER vs. distance and frame size for rate 220 Mbps, CM1 scenario. b) Relative error committed by regression analysis.

In particular, for the CM1 scenario, the terms of matrix B are polynomials of degree 4:

$$\begin{aligned} &b_{0,0}(r) = 2.06\cdot10^{-7}r^4 - 1.53\cdot10^{-4}r^3 + 2.81\cdot10^{-2}r^2 - 1.58\,r + 25.36; \\ &b_{0,1}(r) = -1.09\cdot10^{-9}r^4 + 8.39\cdot10^{-7}r^3 - 1.66\cdot10^{-4}r^2 + 9.62\cdot10^{-3}r - 0.16; \\ &b_{0,2}(r) = 5.18\cdot10^{-13}r^4 - 3.93\cdot10^{-10}r^3 + 7.52\cdot10^{-8}r^2 - 4.30\,r + 6.98\cdot10^{-5}; \\ &\vdots \end{aligned} \qquad (13)$$

The goodness of this fit is confirmed by the observed value of the *determination coefficient* R^2 over polynomial function: in fact the minimum observed value of R^2 is 0.9944 for r=500 Mbps. Another parameter that confirms the accuracy of regression is the relative error: in this case the maximum value observed on all rates is 6.9639% still for r=500 Mbps.

If we fix the value of r to 220 Mbps in eq.10, we obtain the following elements for B:

$$B(220) = B_1 = \begin{bmatrix} -110.60 & 3.1567\cdot10^{-1} & -2.0664\cdot10^{-4} \\ 63.937 & -1.8994\cdot10^{-1} & 1.2444\cdot10^{-4} \\ -14.402 & 4.3882\cdot10^{-2} & -2.8800\cdot10^{-5} \\ 1.5601 & -4.8330\cdot10^{-3} & 3.1776\cdot10^{-6} \\ -8.1214\cdot10^{-2} & 2.5453\cdot10^{-4} & -1.6761\cdot10^{-7} \\ 1.6308\cdot10^{-3} & -5.1545\cdot10^{-6} & 3.3985\cdot10^{-9} \end{bmatrix} \qquad (14)$$

which, substituted in (12), leads to:

$$\begin{aligned} &FER\ (d,p,220) = 10^{\left(\left[B_1\cdot\langle p\rangle_2^T\right]\langle d\rangle_5^T\right)}, \\ &1m < d \le 15m\ ,\ 128bytes \le p \le 1024bytes \end{aligned} \qquad (15)$$

In Fig.5a the FER curve plotted using equation (15) is shown. The observed value of R^2 is in this case 0.9987. The relative error committed by regression analysis is plotted in Fig.5b (in this case the maximum relative error is 6.6298%).

For the CM2 scenario, we have still obtained for the terms of matrix B polynomials of degree 4:

$$\begin{aligned} &b_{0,0}(r) = 3.66\cdot10^{-7}r^4 - 2.79\cdot10^{-4}r^3 + 5.41\cdot10^{-2}r^2 - 3.11\,r + 50.06; \\ &b_{0,1}(r) = -2.07\cdot10^{-9}r^4 + 1.65\cdot10^{-6}r^3 - 3.49\cdot10^{-4}r^2 + 2.08\cdot10^{-2}r - 0.344; \\ &b_{0,2}(r) = 1.50\cdot10^{-12}r^4 - 1.19\cdot10^{-9}r^3 + 2.51\cdot10^{-7}r^2 - 1.50\,r\cdot10^{-5} + 2.47\cdot10^{-4}; \\ &\vdots \end{aligned} \qquad (16)$$

In this case the minimum observed value of R^2 is 0.9945 for the data rate r=500 Mbps. The goodness of this regression is also confirmed by the relative error observed: in fact, the maximum value observed on all rates is 6.6193% still for r=500 Mbps.

For example, if we fix the value of r to 110 Mbps in equation (16), we obtain the following elements for B:

$$B(110) = B_3 = \begin{bmatrix} 44.867 & -3.8570\cdot10^{-1} & 2.7482\cdot10^{-4} \\ -84.848 & 4.2949\cdot10^{-1} & -3.0009\cdot10^{-4} \\ 35.090 & -1.5531\cdot10^{-1} & 1.0782\cdot10^{-4} \\ -6.3834 & 2.6550\cdot10^{-2} & -1.8367\cdot10^{-5} \\ 5.8957\cdot10^{-1} & -2.3640\cdot10^{-3} & 1.6312\cdot10^{-6} \\ -2.7122\cdot10^{-2} & 1.0611\cdot10^{-4} & -7.3061\cdot10^{-8} \\ 4.9390\cdot10^{-4} & -1.8980\cdot10^{-6} & 1.3045\cdot10^{-9} \end{bmatrix} \quad (17)$$

which, substituted in (12), leads to:

$$FER(d,p,110) = 10^{\left(\left[B_3\cdot(p)_2^T\right]\cdot(d)_6^T\right)}, \quad (18)$$
$$1m < d \le 15m \ , \ 128bytes \le p \le 1024bytes$$

The FER course plotted using (18) is shown in Fig.6a. We can see in Fig.6b how the polynomial approximation provided by (18) is excellent because we make a very low maximum relative error (only 0.000017%). This trend is also confirmed by the observed value of R^2 that is 0.9999.

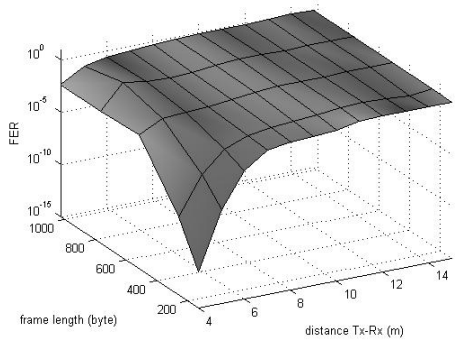

(a)

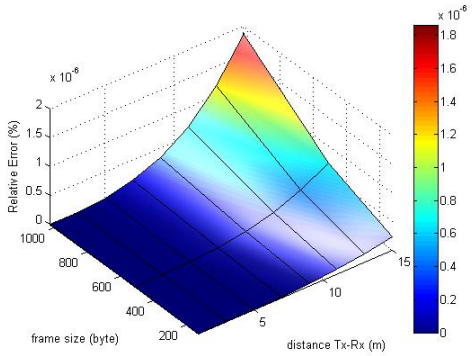

(b)

Fig.6.a) FER vs. distance and frame size for rate 110 Mbps, CM2 scenario. b) Relative error committed by regression analysis.

5. Conclusions

In this paper, we implemented the physical layer of the standard DS-UWB 802.15.3a [2]. Simulation results show how the performances, in terms of FER, of the UWB system, for high data rate degrades for increasing distance (1-15m) and depend also on the frame length. In particular, 28Mbps and 55Mbps rates are slightly influenced by transmitter-receiver distance, especially for CM1. This is due to the low sensitivity to inter-symbol interference. On the other hand, higher data rates (mostly rate ≥220 Mbps) are more sensitive to the transmitter-receiver distance and they can be supported for a shorter distance (in particular this distance decreases for the CM2, CM3 scenario). Moreover, the frame size especially influences the higher data rate, while lower data rate are less sensitive to this factor. This trend is observed mostly for the CM1 scenario, while in the presence of a CM2 scenario there is a general worsening of performance at an increase in the frame size also for the lower data rates. As a result, if the frame length is raised, there is a reduction of the operative range that, in some cases, can be very sensitive.

However, our main contribution is to provide FER analytic expressions for each scenario (in this paper we show only the formulas for the CM1 and CM2 scenarios), expressing it as a function of the data rate, frame size and distance between transmitter and receiver. In this way, a good tool is provided, usable for future applications, which allows the FER to be obtained directly solving a three variables polynomial formula. In order to achieve this purpose, we carried out a three-dimensional regression analysis on obtained simulation results utilizing the specific Mathworks's Matlab fitting tool.

6. References

[1] J. D. Taylor, "Introduction to Ultra Wideband Radar System", *Boca Raton, FL:* CRC, 1995.

[2] www.ieee802.org/15/pub/TG3a.html .

[3] Reed R. Fisher et al., "DS-UWB physical layer submission to 802.15 taskgroup 3a", *IEEE P802.15-04/0137r3*, July 2004.

[4] Oh-Soon Shin, Saeed S. Ghassemzadeh, Larry J. Greenstain and Vahid Tarokh, "Performance Evaluation of MB-OFDM and DS-UWB System for Wireless Personal Area Networks", *IEEE International Conference on Ultra-Wideband*, pp. 214-219, September 2005.

[5] S. Ghassemzadeh, R. Jana, C. Rice, W. Turin, and V. Tarokh, "Measurement and modeling of an ultra-wide bandwidth indoor channel," *IEEETransaction on Commun*., pp. 1786–1796, 2004.

[6] A. Saleh and R. Valenzuela, "A statistical model for indoor multipath propagation", *IEEE J. Select. Areas Commun*., vol. 5, pp. 128-137, Feb. 1987.

[7] Floriano De Rango, Peppino Fazio, Fiore Veltri and Salvatore Marano, "Distance-Dependent BER Evaluation of DS-SS IEEE 802.15.3a Physical Layer under Multiple User Data-Rates and Multi-User Interference", *13th International Conference on Telecommunications*, May 2006.

[8] J. Foerster, "Channel modeling sub-committee report final", *IEEE P802.15-02/490rl*, Feb. 2003.

[9] Qinghua Li, Member, IEEE, and Leslie A. Rusch, Senior Member, IEEE, "Multiuser Detection for DS-CDMA UWB in the Home Environment", *IEEE Jourrnal on Selected Areas in Communications*, vol. 20, NO. 9, December 2002.

[10] A. Parihar, L. Lampe, R. Schober and C. Leung, "Analysis of Equalization for DS-UWB System", *IEEE International Conference on Ultra-Wideband*, pp. 170-175, September 2005.

[11] Ramin Khalili, Kavé Salamatian, "Evaluation of Packet Error Rate in Wireless Networks", MSWIM - Symposium on Modeling, Analysis and Simulation of Wireless and Mobile Systems,Venice, Italy - October, 2004.

[12] C. Montgomery, "Applied Statistics and Probability for Engineers", *Third Edition*, *Wiley*, 2003.